Relic populations of *Fukomys* mole-rats in Tanzania: description of two new species *F. livingstoni* sp. nov and *F. hanangensis* sp. nov

Chris G Faulkes Corresp., [1] , **Georgies F. Mgode** [2] , **Elizabeth Archer** [1] , **Nigel C. Bennett** [3]

[1] School of Biological & Chemical Sciences, Queen Mary, University of London, London, UK

[2] Pest Management Centre, Sokoine University of Agriculture, Morogoro, Tanzania

[3] Department of Zoology & Entomology, University of Pretoria, Pretoria, Gauteng, South Africa

Corresponding Author: Chris G Faulkes
Email address: c.g.faulkes@qmul.ac.uk

Previous studies of African mole-rats of the genera *Heliophobius* and *Fukomys* (Bathyergidae) in the regions of East and south central Africa have revealed a diversity of species and vicariant populations, with patterns of distribution having been influenced by the geological process of rifting and changing patterns of drainage of major river systems. This has resulted in most of the extant members of the genus *Fukomys* being distributed west of the main Rift Valley. However, a small number of isolated populations are known to occur east of the African Rift Valley in Tanzania, where *Heliophobius* is the most common bathyergid rodent. We conducted morphological, craniometric and phylogenetic analysis of mitochondrial cytochrome b (*cyt b*) sequences of two allopatric populations of Tanzanian mole-rats (genus *Fukomys*) at Ujiji and around Mount Hanang, in comparison with both geographically adjacent and more distant populations of *Fukomys*. Our results reveal two distinct evolutionary lineages, forming monophyletic clades that constitute previously unnamed species. Here, we formally describe and designate these new species *F. livingstoni* and *F. hanangensis* respectively. Molecular clock-based estimates of divergence times offer strong support for the hypothesis that vicariance in the Western Rift Valley has initially subdivided populations of mole-rats. Subsequent climatic changes and tectonic activity in the “Mbeya triple junction” and Rungwe volcanic province between Lakes Rukwa and Nyasa have played a role in further isolation of these extra-limital populations of *Fukomys* in Tanzania.

Relic populations of *Fukomys* mole-rats in Tanzania: description of two new species *F. livingstoni* sp. nov. and *F. hanangensis* sp. nov.

Chris G. Faulkes[1], Georgies F. Mgode[3], Elizabeth Archer[1] and Nigel C. Bennett[2]

[1]Queen Mary University of London, School of Biological and Chemical Sciences, UK

[2]Department of Zoology and Entomology, University of Pretoria, South Africa

[3]Pest Management Centre, Sokoine University of Agriculture, Morogoro, Tanzania

Corresponding author: Chris G. Faulkes, Queen Mary University of London, School of Biological and Chemical Sciences, Mile End Road, London E1 4NS. Fax. 020 8983 0973. e-mail c.g.faulkes@qmul.ac.uk

Running title: Tectonics and phylogeography of Tanzanian mole-rats

Abstract

Previous studies of African mole-rats of the genera *Heliophobius* and *Fukomys* (Bathyergidae) in the regions of East and south central Africa have revealed a diversity of species and vicariant populations, with patterns of distribution having been influenced by the geological process of rifting and changing patterns of drainage of major river systems. This has resulted in most of the extant members of the genus *Fukomys* being distributed west of the main Rift Valley. However, a small number of isolated populations are known to occur east of the African Rift Valley in Tanzania, where *Heliophobius* is the most common bathyergid rodent. We conducted morphological, craniometric and phylogenetic analysis of mitochondrial cytochrome b (*cyt b*) sequences of two allopatric populations of Tanzanian mole-rats (genus *Fukomys*) at Ujiji and around Mount Hanang, in comparison with both geographically adjacent and more distant populations of *Fukomys*. Our results reveal two distinct evolutionary lineages, forming monophyletic clades that constitute previously unnamed species. Here, we formally describe and designate these new species *F. livingstoni* and *F. hanangensis* respectively. Molecular clock-based estimates of divergence times offer strong support for the hypothesis that vicariance in the Western Rift Valley has initially subdivided populations of mole-rats. Subsequent climatic changes and tectonic activity in the "Mbeya triple junction" and Rungwe volcanic province between Lakes Rukwa and Nyasa have played a role in further isolation of these extra-limital populations of *Fukomys* in Tanzania.

Introduction

African mole-rats of the family Bathyergidae are subterranean rodents that occur throughout sub-Saharan Africa (Faulkes and Bennett, 2013), with much of their range subdivided by the Great Rift Valley. They have been widely studied as a result of the variation in their social and reproductive strategies, and comparative studies have become crucial in this respect (Allard and Honeycutt, 1992; Faulkes *et al*., 1997; Faulkes and Bennett, 2013). More recently the naked mole-rat (*Heterocephalus glaber*) has also emerged as a model species for the study of longevity and cancer resistance (Gorbunova *et al*., 2014). Hence a clear understanding of their taxonomy, biodiversity and phylogenetic relationships has become increasingly important, not least because they are a speciose group, but also because there are a number of genetically unique, disjunct populations that are limited in their distributional range (Faulkes *et al*. 2004; Ingram *et al*. 2004; Van Daele *et al*. 2007a, b). Historically, systematics of the group has been problematic, because cryptic diversity is prevalent in mole-rats due to convergent morphological evolution of a phenotype adapted to the subterranean niche. However, molecular phylogenies based on both nuclear and mitochondrial genes have produced congruent trees (e.g. Allard and Honeycutt 1992; Faulkes *et al*. 1997; Walton *et al*. 2000; Huchon and Douzery, 2001; Faulkes *et al*. 2004; Ingram *et al*. 2004; Van Daele *et al*. 2007a, b).

Plate tectonics and the formation of the Great Rift Valley have played a central role in the adaptive radiation and distribution of the Bathyergidae, particularly among mole-rats of the genera *Heliophobius* and *Fukomys* (Faulkes *et al*., 2004, 2010, 2011). These taxa are distributed widely, with virtually all members of the genus *Fukomys* occurring in locations west of the Western (Albertine) and Southern Rift Valleys from northern South Africa, through south-central Africa to Uganda and Sudan. South-central Zambia in particular is a hot-spot for species/karyotypic diversity in *Fukomys*, possibly as a result of changing patterns

of drainage over geological time (Van Daele *et al*. 2004, 2007a, b). Disjunct populations are found in Ghana, Cameroon and Nigeria, and a small number of isolated populations occur east of the Rift Valley in Tanzania, where the silvery mole-rat *Heliophobius* is widespread and the predominant bathyergid rodent (Faulkes *et al*., 2011).

Faulkes *et al*. (2010) investigated a number of populations of *Fukomys* (or *Cryptomys sensu lato*) in Tanzania in an attempt to clarify their taxonomic status and to confirm the nomenclature proposed by the earliest reports published by Allen and Loveridge (1933). The latter originally described a new taxon (*Cryptomys hottentotus occlusus*) from Kigogo in south-western Tanzania, interpreting it as a locally adapted form of *Cryptomys hottentotus whytei* (*Fukomys whytei* stricto sensu; Van Daele *et al*., 2007a), which is geographically the closest in distribution to *C. h. occlusus*. Allen and Loveridge also report catching *F. whytei* (*stricto sensu*) from further north at Ujiji. An additional two, more distant locations (Mount Hanang and Liwale), were later recorded for *C. h. occlusus* by Swynnerton and Hayman (1951) in their checklist of Tanzanian mammals. The study by Faulkes *et al*. (2010) concluded that *Fukomys whytei* constitutes a clear phylogenetic species, supporting the monophyletic "*whytei*" clade described by Van Daele *et al*., (2007a), and that *C. hottentotus occlusus* (*sensu* Allen & Loveridge, 1933) should be subsumed into *F. whytei* or, at most, considered a subspecies. With regard to animals sampled from populations at Liwale and Hanang, the former were found to be *Heliophobius* rather than *Fukomys* (Faulkes *et al*., 2011), while genetic analysis of two mole-rats from Hanang appeared to constitute a previously unrecognised species (Faulkes *et al*., 2010). At the time it was not possible to obtain samples from the remaining sites at Ujiji described by Allen and Loveridge.

Here, using molecular phylogenetic and morphometric techniques we characterize fully and name a new species from the population of mole-rats in the Hanang region, extending the sampling north to include neighbouring populations at Mbulu. We also

investigate for the first time mole-rats collected near Ujiji, and in doing so describe and name a second new species.

Methods

Sampling, PCR and sequencing

Samples were obtained from three main locations in Tanzania between August 2006 and July 2013 (Ujiji: n=6, Hanang: n=9 and Mbulu: n=31), to compare with other geographically relevant material already collected and sequenced (Faulkes *et al*., 2004; Van Daele *et al*., 2007; Table 1, Figure 1). Tissue (muscle or skin biopsies and whole animals) was fixed in 95% ethanol and then stored at –20ºC prior to DNA extraction and/or morphological analysis. Genomic DNA was extracted from the tissue samples and PCR amplification of the entire cytochrome *b* (*cyt b*) gene (1140 bp) carried out using primers and protocols previously described for African mole-rats by Faulkes *et al*. (1997). Sequencing was carried out in both directions using combinations of primers to obtain complementary partially overlapping strands (20-100% overlap), using the Eurofins Genomics Value Read automated sequencing service (Eurofins Genomics, Ebersberg, Germany).

Ethical note

Animals were euthanised with an overdose of chloroform on the day of capture. Sexing, weighing and tissue collection were carried out post mortem. Fieldwork was funded and approved by the University of Pretoria, Animal Use & Care Committee Approval EC053-09. Sampling focused around agricultural areas where mole-rats are considered pests. Collection permits were issued by the Sokoine University of Agriculture and respective District Authorities (Hanang, Mbulu and Ujiji). The Tanzania Commission for Science and Technology (COSTECH) granted a research permit for collection of rodents (permit no.

116 2013-260-NA-2014-110) to Dr. Georgies Mgode. Export permits were obtained from the
117 Wildlife Department (Ministry of Natural Resources and Tourism Tanzania), and
118 Zoosanitary/Veterinary permit from the Ministry of Livestock Development and Fisheries.
119

120 **Analysis of mitochondrial DNA sequences**

121 Sequences were aligned manually for analysis using Mesquite version 3.03 (Madison and
122 Madison, 2014) and phylogenetic relationships investigated using a standard range of
123 parsimony, maximum likelihood and Bayesian approaches. Maximum Likelihood fits of 24
124 different nucleotide substitution models were used to establish the evolutionary model most
125 appropriate for the data (from Hierarchical Likelihood Ratio tests), and these parameters were
126 then used in subsequent analyses, where appropriate. Maximum likelihood and parsimony
127 analyses were undertaken and phylogenetic trees and genetic distances among haplotypes
128 based on nucleotide sequences constructed using MEGA 6 (Tamura *et al*., 2013). Maximum
129 likelihood was conducted using the heuristic search option, with initial tree(s) for the search
130 obtained automatically by applying the Maximum Parsimony method. For maximum
131 parsimony we used the min-mini heuristic algorithm with a search factor of 1 with gaps
132 treated as missing data and eliminated from the analysis. Bootstrap analysis was conducted
133 with 100 replicates of the dataset.

134 Bayesian phylogenetic analysis was undertaken using BEAST v1.8.2 (Drummond *et*
135 *al*., 2007, 2012). Following the molecular clock likelihood ratio test performed using MEGA
136 6 (Tamura *et al*., 2013) to establish the correct molecular clock model, the null hypothesis of
137 equal evolutionary rate throughout the tree was rejected (likelihood ratio = 9.92; $P > 0.001$).
138 Thus an uncorrelated relaxed molecular clock model (Drummond *et al*., 2006) and a Yule
139 tree prior (the most suitable for interspecies comparisons) were selected in BEAST, and an
140 HKY model of molecular evolution. The molecular clock rate was calibrated by assuming a

141 divergence time of 10-11 Mya for the common ancestor of *Cryptomys*/*Fukomys* (the ingroup
142 in this study), and these divergence times for the ingroup were input as a prior with upper
143 (11) and lower (10) limits. This calibration has been previously used by Ingram *et al*. (2004),
144 Van Daele *et al*. (2007a) and Faulkes *et al*. (2010), and was based on a timing of 19 Mya for
145 the divergence of the *Heliophobius* lineage within the bathergid family tree, and the
146 occurrence of the fossil *Proheliophobius* (Lavocat, 1973). After initial data exploration with
147 independent chains we implemented a final run having a chain length of 30,000,000,
148 sampling output every 30,000 iterations. The first 300,000 trees (10%) were discarded during
149 burn-in. Mixing and convergence of MCMC chains generated by BEAST were investigated
150 and checked using Tracer v1.6.0 to ensure sufficient iterations and sampling were performed
151 before samples from the posterior distribution of trees were summarized using Treeannotator
152 v1.8.2, and trees drawn using FigTree v.1.4.2 (Drummond *et al*., 2012).

153 Each distinct haplotype obtained from the two geographical locations (Ujiji and
154 Hanang) were included in all phylogenetic analyses, together with the published sequences
155 representative of the main clades of *Fukomys* (Van Daele *et al*. 2007a; Faulkes *et al*., 2010),
156 and two other bathyergid mole-rats as outgroups: *Cryptomys hottentotus hottentotus* and
157 *Heliophobius emini* (Faulkes *et al*., 2011). In addition, a previously unpublished *Fukomys*
158 sequence from Ghana was included as another example of an extralimital, but geographically
159 distant population.

160

161 **Morphology, craniometrics and analysis of skull shape**

162 Pelage colour was recorded under natural daylight by consensus of three observers, with
163 reference to Munsell Soil Color Charts (1954 Edition; Munsell Color Co., Inc. Baltimore,
164 USA). Subsequent descriptions of colour all refer to this scale. Morphometric measurements
165 were taken from a total of 31 skulls (26 Hanang region; 5 Ujiji) using digital callipers (to the

166 nearest 0.1 mm), as described by Verheyen *et al*. (1996) (Figure S1), together with standard
167 head, body, tail and hind foot length measurements, in specimens where the entire body was
168 available. Age classes were estimated from tooth eruption and wear characteristics as
169 previously described for *Fukomys damarensis* (Bennett *et al*., 1990).
170 In order to investigate and quantify any differences in skull morphometrics between *Fukomys*
171 *livingstoni* and *Fukomys hanagensis*, shape variation was investigated using landmark
172 analysis, as previously described in Faulkes *et al*. (2010). The dorsal and ventral surfaces of
173 skulls from specimens collected at Hanang (n=2), Mbulu (n=24), Ujiji (n=5), and Kigogo (*F*.
174 *whytei*, the geographically closest species; n=3), were photographed three times to minimize
175 the effects of misalignment. For further comparison, material (n=20) from *F*. *whytei* was
176 obtained in the form of photographs of the dorsal and ventral surfaces of the skulls collected
177 by Allen & Loveridge (1933), and were provided by the Harvard Museum of Comparative
178 Zoology (see Faulkes *et al*., 2010 for further information). In addition, photographs of the
179 dorsal and ventral surfaces of the skulls from the more geographically remote *F*. *anselli*
180 (n=20) from Lusaka, Zambia were also included. The relative locations of these samples are
181 displayed in Figure 1. To capture the shape, the 2-D coordinates of a total of 15 dorsal and 17
182 ventral landmarks as previously described in Faulkes *et al*. (2010; Figure S2) were placed on
183 each photograph and digitized using the TpsDIG2 software (Version 1.4; Rolf, 2004), and
184 mean relative warp scores for each specimen produced by tpsRelW (Version 1.36; Rolf,
185 2003) were plotted.
186
187 **New Zoological Taxonomic Names**
188 The electronic version of this article in Portable Document Format (PDF) will represent a
189 published work according to the International Commission on Zoological Nomenclature
190 (ICZN), and hence the new names contained in the electronic version are effectively

191 published under that Code from the electronic edition alone. This published work and the
192 nomenclatural acts it contains have been registered in ZooBank, the online registration
193 system for the ICZN. The ZooBank LSIDs (Life Science Identifiers) can be resolved and the
194 associated information viewed through any standard web browser by appending the LSID to
195 the prefix http://zoobank.org/. The LSID for this publication is:
196 [urn:lsid:zoobank.org:pub:DC6D5104-CB60-48A1-9A06-B16A25DC6573]. The online
197 version of this work is archived and available from the following digital repositories: PeerJ,
198 PubMed Central and CLOCKSS.
199
200 **Results**
201 **General capture information**
202 Ujiji
203 A total of six animals were sampled from two sites 1.5 km apart and at an altitude of 2601 to
204 2624 m above sea level, at Msimba Village on the outskirts of Ujiji (Table 1; Figure 1a,b).
205 The capture sites were either in or directly adjacent to fields containing maize, sweet potato,
206 cassava, palms and bananas. At one location at Site 1 (Msimba village, Kasaka hamlet), an
207 adult male and young female were captured from the same trap (NHMUK 2015.42 and
208 NHMUK 2015.43), with an adult male (NHMUK 2015.46) trapped a few metres away and
209 likely from the same burrow. An adult female and a young male (NHMUK 2015.44 and
210 NHMUK 2015.45) were caught at further locations nearby (115 m distant) at Site 1 and may
211 represent different colonies. All individuals had the same *cyt b* Haplotype "D". At Site 2
212 (Msimba village, Kabemba site), a single adult male (NHMUK 2015.47) was caught at 2601
213 m above sea level in a valley with sweet potato fields and uncultivated grassland. This
214 individual was assigned to a different *cyt b* Haplotype "E".
215

Hanang/Mbulu

At Hanang, 640 km east and slightly north of Ujiji, nine animals were collected from two sites around Hanang Mountain at altitudes of 1856 to 1957 m above sea level: at Gitting Village and at Jorodom Village, 8 km SW from Gitting (Table 1; Figure 1a,c). The capture sites were either in uncultivated grassland adjacent to or on the edge of fields next to cultivated mixed crops, bananas and planted trees. A single individual each had Haplotype A or Haplotype B at Gitting, while the remaining six at Gitting and two at Jorodom Village had Haplotype B (Table 1; Figure 1).

Further north thirty-one animals were collected at altitudes of 2115 to 2188 m above sea level from seven distinct catching sites/colonies from another population at Mbulu, 42 km north of Gitting Village (Hanang). Habitat at Mbulu was similar to that around Hanang, either in uncultivated grassland adjacent to or on the edge of fields next to cultivated mixed crops (e.g. potatoes, maize, sugarcane, and bananas). From one to eight individuals were caught at the seven colony sites (Table 1). All twenty of the thirty-one animals sequenced from the Mbulu population had the same Haplotype "C".

Phylogenetic relationships

The maximum likelihood tree with the highest log likelihood (-5146.172) is shown in Figure 2a. Initial trees for the heuristic search were obtained automatically by applying the maximum parsimony method. A discrete Gamma distribution was used to model evolutionary rate differences among sites (5 categories (+G, parameter = 0.453)). The rate variation model allowed for some sites to be evolutionarily invariable ([+I], 52.275% sites; Tamura & Nei, 1993; Tamura *et al*., 2013). Bootstrap support was high for the main taxonomic groupings (80-100%), with the exception of Lufubu (69%), although the latter was consistently placed as the sister group to the East Bangweulu clade in all trees.

Maximum parsimony analysis produced four trees of length 883 (Figure 2b; consistency index = 0.466; retention index = 0.612). From the total of 1140 characters, 674 were constant, 325 variable characters were parsimony informative and 141 uninformative. One of the trees (Figure 2b (i)) was identical to the maximum likelihood tree. The other three most parsimonious trees differed in the relative placement of the *whytei* clade with respect to Lufubu, East Bangweulu, West Bangweulu and *amatus* clades, and the swapping of lineages of *F. whytei* from Mbala and Kigogo within the *whytei* clade (Figure 2b (ii), (iii) and (iv)).

Bayesian phylogenetic analysis performed with BEAST produced a tree identical to maximum likelihood tree 2a and maximum parsimony tree 2b (i), with all nodes having high posterior support (0.86 to 1.00/86-100%; Figure 3).

Maximum likelihood, maximum parsimony and Bayesian trees were all congruent in supporting previously accepted taxonomic groupings (*whytei*, Lufubu, East Bangweulu, West Bangweulu, *amatus*, *darlingi*, *damarensis*, *micklemi*, *bocagei*, *mechowii*, and *vandewoestijneae*; Van Daele *et al*. 2007a, b; Faulkes *et al*., 2010). The sequence of *F. zechi* from Ghana formed an early diverging lineage in the *Fukomys* clade, supporting previous studies that extra-limital populations of *Fukomys* in west and central Africa represent relic populations from an initial radiation of ancestral *Fukomys* (Ingram *et al*., 2004). Next a clade containing *F. mechowii*, *F. bocagei* and the recently described *F. vandewoestijineae* (Van Daele *et al*., 2013) constitute a group of species distributed through central and west central Africa (Zambia and Angola), and are immediately basal to the populations found at the geographically distant Ujiji. All trees consistently placed the animals collected from Ujiji and Hanang/Mbulu in reciprocally monophyletic clades, separated by the divergence of a major clade containing *F. darlingi*, *F. damarensis*, and *F. micklemi*/*F. kafuensis*. Finally, a monophyletic group containing five distinct clades was consistently recovered (West Bangweulu, *F. amatus*, Lufubu, East Bangweulu and *F. whytei*; Figure 2).

The phylogenetic analysis provides robust evidence for two hitherto unrecognised phylogenetic species in Tanzania, one from Ujiji (*Fukomys livingstoni sp. nov.*) and a second from the Hanang/Mbulu region (*Fukomys hanangensis sp. nov.*). Both were genetically divergent from one another within the molecular phylogeny for the *Fukomys* genus, and also from the geographically closest clade containing *F. whytei*. Each of the *Fukomys sp. nov.* form monophyletic clades strongly supported by bootstrap values of 100% (maximum likelihood) and posterior probabilities of 1.00 (Bayesian trees).

Inter-clade sequence divergence

Maximum Likelihood fits of 24 different nucleotide substitution models indicated that the Tamura-Nei + G + I (TN93+G+I) model of sequence evolution was the most appropriate. Both mean uncorrected-*p* and TN93+G+I corrected genetic distances between lineages/clades represented in Figures 2 and 3 are displayed in Table 2. Uncorrected *p* (and (TN93+G+I) distances between *F. hanangensis* and ingroup lineages from different locations ranged from a minimum of 6.3% (7.0%) versus the Lufubu clade to 14.5% (18.5) versus *F. zechi*. Uncorrected *p* distances between *F. livingstoni* and ingroup lineages ranged from a minimum of 8.5% (9.8) versus *F. amatus* to 14.5% (18.8) versus *F. zechi*. Mean *p* distance between *F. livingstoni* and *F. hanangensis* was also 8.5% (9.9), while *p* distances between these and the geographically closest *F. whytei* clade were 9.7% (11.6) and 6.5% (7.3) respectively, exceeding the distances among some currently recognised species, e.g. *F. amatus* and *F. whytei* 4.7% (5.9%). Genetic distances between haplotypes within *F. hanangensis* and *F. livingstoni* clades were very low. For the three *F. hanangensis* haplotypes (A, B and C) the total number of substitutions over the 1140 bp (and uncorrected *p* distances) were A versus B: 1 (0.001%), A versus C: 4 (0.004%), and B versus C: 3 (0.003%). For the two *F.*

290 *livingstoni* haplotypes D and E the total number of substitutions over the 1140 bp (and
291 uncorrected *p* distances) were: 6 (0.007%).
292
293 **Molecular clock estimates of divergence times and phylogeographic trends**
294 Figure 4 summarises the molecular clock-based divergence times, together with 95%
295 highest posterior density (HPD) intervals (equivalent to 95% confidence intervals), for the
296 main nodes within the phylogeny generated using BEAST. According to the maximum clade
297 credibility tree produced by BEAST (Figure 3) the divergence of the Ujiji lineage and *F.*
298 *livingstoni* (Node A in Figure 3) occurred in the Pliocene at 3.55 Mya, with a 95% HPD
299 extending into the Early Pleistocene (representing 2.63 to 4.89 Mya). Following the common
300 ancestor of the *darlingi*, *damarensis* and *micklemi* clades with species now extant in south
301 central Africa, the divergence of the Hanang/Mbulu lineage and *F. hanangensis* (Node B in
302 Figure 3) is estimated at 2.36 Mya in the Pleistocene (lower and upper bound of the 95%
303 HPD = 1.68 - 3.25 Mya). Thus the timings of divergence of both the Ujiji and Hanang/Mbulu
304 lineages precede the commencement of increased tectonic activity at the Mbeya Triple
305 Junction (MJT; Figure 3), which forms the conduit between south central Africa and
306 Tanzania. A sister group to *F. hanangensis* contains five clades with taxa restricted to
307 Zambia, with the exception of the *F. whytei* clade (red circles in Figure 1a), which includes
308 lineages that diverged much more recently in the Pleistocene. Geographically these
309 populations of *F. whytei* are concentrated around the MTJ region, with only Kigogo
310 population significantly within Tanzania. There was no consistent geographical structuring of
311 the main clades in the phylogeny in any of the analyses.
312
313 **Morphometric analysis of skulls**

Morphometric analysis of *F. livingstoni* and *F. hanangensis*, together *F. whytei* from south western Tanzania and *F. anselli* from Lusaka, Zambia, differentiated skulls in line with the proposed taxonomy, when relative warps 1 and 2 from either or both the dorsal and ventral surfaces were plotted (Figure 4a,b). For example, the dorsal surface analysis clearly separates *F. livingstoni* and *F. anselli* from each other, and from an unresolved cluster of points from *F. hanangensis* and *F. whytei* skulls. The ventral surface differentiates all four taxa, although there is a small overall between *F. livingstoni* and *F. hanangensis*. The overall skull shape changes occurring along the relative warp axes are captured in thin plate spline plots in Figure S3 (dorsal surface) and Figure S4 (ventral surface).

The clear separation of the *F. livingstoni* samples from the consensus shape (corresponding to the origin in the plot in Figure 4a) and the *F. hanangensis*/*F. whytei* morphospace, along relative warps 1 and 2 of the dorsal surface is due to three main effects: (i) anterior-medial shifting of the jugal within the zygomatic arch (landmarks 4 and 6), (ii) shortening of the nasal bones, particularly at their posterior extent (landmarks 1, 2, 14 and 15), and (iii) anterior/anterior-medial shifts in the parietal (landmarks 8, 9 and 12; Figures S2 and S3). To some extent these same changes occur when moving from the *F. hanangensis*/*F. whytei* morphospace (i.e. upper right quadrant of Figure 4a) to *F. anselli* (upper left quadrant of Figure 4a), as this is also a shift along the x-axis. The additional separation of *F. livingstoni* and *F. anselli* points along the y-axis result from a posterior-lateral shifts in the narrowest inflection of squamosal (landmark 10) and the right anteriolateral tip of the parietal bone (landmark 9), and a posterior-medial shift in the anterior tip of the interparietal bone (landmark 11).

On the ventral skull surface, changes in *F. livingstoni* from the consensus shape (and *F. hanangensis*) are principally due to small a lateral shift in the posterior tip of auditory bulla at the junction with the occipital (landmark 9) and a small anterior-medial shift in the

339 junction of the jugal and zygomatic process (landmark 4). These changes are present, but less
340 exaggerated, in *F. whytei*, which also occupies the morphospace in the upper right quadrant
341 of the relative warp plot (Figure S4). Changes from the consensus shape in the main group of
342 *F. hanangensis* points were small as they cluster quite close to the origin on the plot. The
343 separation of *F. anselli* along the y-axis results from anterior shifts in both the junction of
344 squamosal and auditory bulla, and the lateral tip of auditory bulla (landmarks 7 and 8), and a
345 posterior shift in the junction of jugal and zygomatic process (landmark 4; Figure S4).

346 Standard craniometric measurements are displayed in Table S1. Because of the small
347 sample size of *F. livingstoni* a comprehensive statistical analysis of craniometrics among
348 sexes, age classes and species was not possible. However, there are some differences
349 apparent, evident from the shape analysis described above (e.g. the anterior-medial shifting of
350 the jugal within the zygomatic arch). For example, the skull of *F. livingstoni* is thus slightly
351 more elongated than *F. hanangensis*. This is evident in the ratio of greatest length of skull
352 (M1 in Figure S1) to zygomatic breadth (M9 in Figure S1), which is significantly higher in *F.*
353 *livingstoni* than *F. hanangensis*: 1.533 ± 0.022 versus 1.469 ± 0.009 respectively (P=0.0078,
354 t=2.858, df=29).

355

356 **Description of species**

357 Family Bathyergidae Waterhouse, 1841

358 Genus *Fukomys* Kock *et al*. 2006

359 ***Fukomys livingstoni*** sp. nov.

360 Livingstone's mole-rat (common name)

361 LSID urn:lsid:zoobank.org:act:67DEACE5-3163-4FAE-885B-8EC04F072EEC

362 **Holotype**

NHMUK 2015.42 is an adult male collected in July 2013 at the Kasaka hamlet within the village of Msimba, near Ujiji. The specimen is composed of a skin and skull in very good condition (Figure 5a,b; Figure 6a). The external measurements (mm) are: head and body length 115.4, tail 8.9 and hind foot 22 (Table 1). The body weight was 50g. The pelage is darkish grey brown overall with a shorter very dark grey under-fur and a small irregularly shaped light grey head patch.

Paratypes

A further five specimens (NHMUK 2015.43 - NHMUK 2015.46) were collected from around the type locality (Table 1; Figure 1a,b).

Etymology

This species is named after Dr. David Livingstone, as Ujiji (the type locality) is the site of the famous meeting on 10 November 1871 when Henry Morton Stanley found the explorer David Livingstone, who many thought to be dead, and uttered the famous words “Dr. Livingstone, I presume?” (Stanley, 1872).

Type locality

Msimba village, 6.4 km northeast from the city centre of Ujiji (S 04º 51.760'; E 029º 42.326'). The specimen was trapped in a valley at an altitude of 793 m (2601 ft) above sea level, in an area with moist sandy soil, where cassava, sweet potato, maize, palms and bananas were being cultivated.

Distribution and biology

The full range of this species remains to be determined with collection of the series described here restricted to around the village of Msimba on the outskirts of Ujiji. The holotype was captured from the same hole in the burrow as a young adult female (NHMUK 2015.43), with an adult male (NHMUK 2015.46) trapped a just few metres away and probably from the same burrow. The presence of adults and young adults together in a burrow suggests natal

388 philopatry and cooperative breeding that is a characteristic of species within the genus
389 *Fukomys*.

390 **Diagnosis**

391 Individuals of this species may be clearly distinguished from adjacent populations of *F.*
392 *hanangensis* and *F. whytei* on the basis of morphology and molecular (DNA sequence) data.
393 Morphologically, *F. livingstoni* is smaller with a mean adult body size (age class 2 and
394 above) of 55 ± 8.9g (n=4) compared with *F. hanangensis* (mean adult body weight = 83.4 ±
395 5.6 g; n=30; Table 1). The skull of *F. livingstoni* is more elongated with a larger ratio of
396 greatest length of skull to zygomatic breadth than *F. hanangensis* due to less curvature of the
397 jugal (Table S1; Figure 6). A head spot (bles) is present in the specimens obtained for this
398 study, although the presence/absence of the bles may not always be a reliable diagnostic
399 feature as there is often intraspecific variation in other bathyergids.

400 **Description (and comparison with other species)**

401 This is a small species of *Fukomys*: the four adults (age classes 2 to 4) ranged from 38-80 g in
402 body weight of (mean = 55.0 ± 8.9g; Table 1), similar in proportion to *F. darlingi* found in
403 Zimbabwe, where mean body weights are 65.3 ± 14.1g (males) and 62.9 ± 14.9 (females;
404 Bennett *et al*., 1994). When compared with other species of *Fukomys* from south-central
405 Africa, the ratio of body length to body weight and the size of the skull (expressed as greatest
406 width/greatest length) is at the lowest end of the distribution, and much smaller than *F.*
407 *damarensis* and *F. mechowii* (Figure S6). Overall pelage colouration varied from darkish
408 grey-brown to brown and dark brown, with shorter under-fur of very dark grey or black. A
409 small irregularly-shaped head spot was present, varying from light grey to white in colour
410 (Table S2; Figure S5a). In this respect *F. livingstoni* is similar to neighbouring *F. whytei*,
411 whose range extends into south-western Tanzania, where a small head spot is reported to be
412 present in some populations (Allen & Loveridge 1933; Burda *et al*., 2005). Otherwise *F.*

413 *livingstoni* is much smaller than *F. whytei*, where body weight means (g) for animals from the
414 type locality of Karonga, Malawi were 132.7 ± 22.3 (males, n=4) and 121.5 ± 10.7 (females,
415 n=4; Burda *et al*., 2005). Specimens of *F. whytei* geographically closer to Ujiji (from Kigogo,
416 Tanzania) were also within this size range, with a young animal of age class 1 (and 3/4 cheek
417 teeth erupted) recorded at 101g, larger than adult *F. livingstoni* (Table 1). To the trained eye,
418 pelage colour may also distinguish the more grey-brown/brown *F. livingstoni* from *F. whytei*,
419 although the latter is reportedly variable among populations from cinnamon-grey to dark
420 slatey (Allen & Loveridge 1933) and grey-buff (Burda *et al*., 2005). Body size also clearly
421 distinguishes *F. livingstoni* from the larger *F. hanangensis* (see below) found further north in
422 Tanzania, and while the latter lacks a paler coloured head spot (at least in the sample set
423 reported here) and tends to be more yellowish brown, there is some overlap in pelage
424 colouration.
425
426
427 Family Bathyergidae Waterhouse, 1841
428 Genus *Fukomys* Kock *et al*. 2006
429 ***Fukomys hanangensis*** sp. nov.
430 The Hanang mole-rat (common name)
431 LSID urn:lsid:zoobank.org:act:59C00958-9628-461F-987D-AB897F52598F
432
433 **Holotype**
434 NHMUK 2015.15 is an adult breeding female, collected in September 2009 from Jorodom
435 village on the slopes of Mount Hanang. The specimen is composed of an entire body
436 preserved in ethanol in very good condition (Figure 5c,d). The external measurements (mm)

437 are: head and body length 111.0, tail 12.2 and hind foot 23.1 (Table 1). The body weight was
438 62g. The pelage is brown overall with a shorter black under-fur. No head spot is present.

439 **Paratypes**

440 A further 40 specimens including 27 paratypes (NHMUK 2015-14 and NHMUK 2015.16 -
441 NHMUK 2015.41) and 13 samples retained at Queen Mary, University of London for further
442 analysis. Eight of these were collected from around the type locality at Hanang, while the
443 remaining 31 were from locations around Mbulu (Table 1; Figure 1a,c).

444 **Etymology**

445 Named after the location where the specimens were first collected around Mount Hanang,
446 Tanzania.

447 **Type locality**

448 Jorodom village, (S 04º 29.510'; E 035º 24.519'). The specimen was trapped in a valley at an
449 altitude of 1957 m (6422 ft) above sea level, in an uncultivated grass field surrounded by crop
450 fields.

451 **Distribution and biology**

452 Currently the range of this species is known to be around Mount Hanang including the
453 villages of Gitting and Jorodom, and extending to at least 40 km further north to Mbulu. The
454 full range of this species remains to be determined. Aside from the first three animals
455 captures in 2006, the remaining 37 specimens collected in 2009 from Gitting, Jorodom and
456 Mbulu were gathered from 10 colonies with up to eight being caught from one burrow
457 (Colony 4 at Tumati-Eyasirong, Mbulu; Table 1). These are not maximum colony sizes as
458 burrows were not completely trapped out, and no breeding females were captured at Mbulu.
459 Specimens from Colony 4 consisted of five males and three females, including a young 35g
460 male of age class 1, and mature adults of age classes 2 and 3. A similar spread of age classes

was also seen among the animals collected from Mbulu Colony 5. These observations suggest natal philopatry and cooperative breeding for this species.

Diagnosis

Individuals of this species may be clearly distinguished from adjacent populations of *F. livingstoni* and the more geographically distant *F. whytei* on the basis of morphology and molecular (DNA sequence) data. Morphologically, *F. hanangensis* is larger than neighbouring *F. livingstoni*, with a mean adult body size (i.e. excluding animals of known age class 1) of 83.4 ± 5.6g (range: 35-140; n=30; Table 1). Compared with *F. livingstoni*, the skull of *F. hanangensis* is wider in appearance with a smaller ratio of greatest length of skull to zygomatic breadth, with a greater curvature of the jugal (Table S1; Figure 6).

Description (and comparison with other species)

F. hanangensis is a small to medium sized example of the genus *Fukomys*, while at an average adult size of 83g it is larger than *F. livingstoni* (mean adult body weight = 55.0 ± 8.9g, range: 38-80g ; n=4; Table 1), it is slightly smaller in proportions to *F. whytei*, where body weight means (g) for animals from the type locality of Karonga, Malawi were 132.7 ± 22.3 (males, n=4) and 121.5 ± 10.7 (females, n=4; Burda *et al*., 2005). In comparison with other species of *Fukomys* from south-central Africa (Figure S6), the ratio of body length to body weight and the size of the skull are smaller than *F. damarensis* and *F. mechowii*. However, it would be hard to distinguish *F. hanangensis* from species such as *F. darlingi*, *F. anselli*, *F. bocagei*, *F. kafuensis* and *F. vandewoestijneae* on the basis of body size alone. There was a trend towards male *F. hanangensis* being larger than females: 90.8 ± 8.0g (n=19) versus 72.5 ± 4.8g (n=10) respectively, although this was not significant (P=0.127, t=1.575, df=27). Overall pelage colouration varied from yellowish brown through dark yellowish brown to brown/dark brown. Under-fur was normally black, with two specimens very dark grey. None of the series described here had a lighter-coloured head spot present (Figure S5b).

Thus *F. hanangensis* can be morphologically distinguished from neighbouring *F. livingstoni* by its larger size and a more yellowy brown coat than *F. livingstoni*, and a lack of lighter head spot.

Discussion

This study builds on preliminary sequence data from two mole-rats collected at Hanang in Tanzania, originally reported by Faulkes *et al*. (2010). Not only do we confirm the presence of a previously unrecognised species of African mole-rat in this region (*Fukomys hanangensis*), but also provide robust evidence for a second new species from specimens collected from a new locale at Ujiji (*Fukomys livingstoni*). We base our descriptions of the new species primarily on genetic data, although clear morphological differences are also evident in skull shape, pelage and body size. Within the genus *Fukomys*, both *F. hanangensis* and *F. livingstoni* are distinct evolutionary lineages, as defined by the Phylogenetic Species Concept (Cracraft 1989), and form separate monophyletic clades nested among other clearly defined species in the *cyt b* molecular phylogeny. An increasing number of single locus mtDNA (in particular *cyt b*) and nuclear gene-based phylogenies have produced robust and consistent phylogenies for the Bathyergidae and clarified the taxonomy of cryptic species (Allard & Honeycutt 1992; Faulkes *et al*., 1997, 2004, 2010, 2011; Walton *et al*., 2000; Huchon & Douzery, 2001; Ingram *et al*., 2004). Indeed, recent phylogenomic analysis of the main lineages within the family using data from 3,999 concatenated genes agree fully with these single gene studies, producing a tree with a congruent topology (Davies *et al*., 2015).

The previously unpublished sequence for *F. zechi* (the Togo mole-rat) from Ghana, which we also include in our phylogeny here, formed a distinct and highly divergent basal lineage within the *Fukomys* clade as a whole. This would place *F. zechi* with the other poorly known extra-limital West and Central African *Fukomys* as relic populations of the initial

radiation of the genus, including *F. foxi* from Cameroon and *F. ochraceocinereus* from South Sudan (Ingram *et al*., 2004).

The divergent nature of *F. hanangensis* and *F. livingstoni* within the topology of the *cyt b* gene tree is also evident in the magnitude of the genetic distances between the clades, adding further support for their evolutionary distinctiveness (and within clade differences between haplotypes were very low). For example corrected *p* distances between geographically adjacent *F. whytei* versus *F. hanangensis* and *F. livingstoni* are 7.3 and 9.7% respectively, while *F. hanangensis* and *F. livingstoni* differ by 8.5%. These values exceed those of recognised species within the *Fukomys* clade, for example *F. amatus* versus *F. whytei* (5.9%), and *F. mechowii* versus *F. vandewoestijneae* (4.8%; Table 2).

It is well established that chromosome number and karyotype vary considerably within *Fukomys*. Unfortunately it was not possible to obtain a karyotype for *F. livingstoni*. However, preliminary studies of one individual *F. hanangensis* indicate that 2n=46 (J. L. Deuve and N. C. Bennett, unpubl. data), the same as that of *F. whytei* collected from the type location of Karonga (Burda et al., 2005). As discussed by Faulkes *et al*., 2010, based on our phylogeny, a karyotype of 2n=46 would appear to be the ancestral state for the clade containing the *F. hanangensis* lineage as the basal group (Figure 2a), this being retained in *F. whytei*, but modified to 2n=50 in *F. amatus* (Macholan *et al*., 1998) and a 2n=64 in populations from Kasama (Kawalika *et al*., 2001). It seems likely that the karyotype of *F. livingstoni* is also different, given the variation among sister groups, for example *F. bocagei*: 2n=58 (G.H. Aguilar *pers. com.*), *F. mechowii*: 2n=40 (Macholan *et al*., 1993), *F. vandewoestijneae*: 2n=44 (Van Daele *et al*., 2013), *F. micklemi*: 2n=60 (Van Daele *et al*., 2004), *F. kafuensis*: 2n=58 (Burda *et al*., 1999), *F. darlingi*: 2n=54 (Aguilar 1993) and *F. damarensis*: 2n=74-78 (Nevo *et al*., 1986).

We have previously drawn attention to the potential role of rifting and volcanic activity in cladogenesis within *Fukomys* (Faulkes *et al*., 2004, 2010), while Van Daele *et al*. (2004, 2007) hypothesise that consequent shifts in the patterns of drainage of major river systems in south-central Africa occurring in the Pliocene/Pleistocene have further subdivided populations of mole-rats. Formation of the African Great Rift Valley began about 50 million years ago (Mya), pre-dating the hypothesised origin of the family Bathyergidae. Later, major rifting occurring in the Miocene, which continued through the Pliocene and Pleistocene and produced the great African lakes, mountains and volcanoes that characterize East Africa (for recent reviews see Chorowicz, 2005 and Macgregor 2015). An area of particular importance to the radiation of *Fukomys* and the new species described in this study are the Western and Southern Rifts. This includes Lakes Tanganyika, Rukwa and Nyasa (Malawi), and the corridor of land between them connecting Zambia, Malawi and Tanzania, geologically known as the Mbeya Triple Junction (MTJ; Figure 1). From at least the early-Pliocene onwards, this area may have constituted the only route for dispersal of terrestrial and subterranean animals, as the Lake Tanganyika basin is thought to have filled to produce a deep lake 6–12 Mya (Cohen *et al*. 1993), while initial rifting in northern lake Nyasa commencing in the Messinian (upper-most Miocene, 7.2-5.3 Mya; Macgregor, 2015) and attained deep-water conditions by 4.5 Mya (Delvaux, 1995, 1998). However, the extent and timing of lake formation in these major rift basins is still controversial, with more recent dates being suggested (see Weiss *et al*., 2015 for recent discussion in the context of Lake Tanganyika cichlids).

In our molecular phylogenetic analysis, there was no consistent geographical structuring of the main clades, with geographically adjacent clades divergent in the gene trees. For example, *F. hanangensis* and *F. livingstoni* while geographically relatively close are separated from one another and nearby *F. whytei* by clades endemic to Zimbabwe (e.g. *F.*

560 *darling*), Zambia, Botswana, Namibia and South Africa (e.g. *F. damarensis*), and Zambia
561 (taxa within the East and West Bangweulu clades; Figures 2 and 3). This suggests a series of
562 temporally distinct radiations, presumably involving local extinctions and replacements. In
563 particular, *F. livingstoni* appears to be a basal lineage that extended into East Africa in the
564 Pliocene/Early Pleistocene (4.89-2.63 Mya, according to the maximum clade credibility tree
565 produced by BEAST), within a large clade with a common ancestor at Node A in Figure 3. *F.*
566 *mechowi*, *F. bocagei* and *F. vandewoestijneae* form an immediate outgroup to *F. livingstoni*,
567 all of which are now distributed further south and west in Zambia, and into Angola in the
568 case of *F. bocagei* (Figure 1). *F. hanangensis* represents a later, second incursion into
569 Tanzania occurring 3.25-1.68 Mya. While Lakes Tanganyika and Nyasa may have formed a
570 deep water barrier before the divergence of the *F. hanangensis* lineage and around the time of
571 the earliest estimate for *F. livingstoni*, the dispersal route from south central Africa to East
572 Africa was possible in the terrestrial corridor between Lakes Rukwa and Nyasa, that now
573 forms the MTJ and Rungwe volcanic province (Branchu *et al*., 2005; Macgregor, 2015; see
574 Figure 1). The MTJ/Rungwe volcanic region is at the intersection of the Livingstone basin
575 that forms the north east extremity of Lake Nyasa, the Rukwa–Songwe basin at the south east
576 extremity of the Rukwa rift and the Usangu rift basin. While rifting and volcanism started in
577 this area about 8.6 Mya and intra-basinal faulting, uplift and volcanism were particularly
578 important in shaping the geology of the region at approximately 2.5 Mya, much of the
579 modern topography was generated from 2 Mya and still continues to the present (Ebinger *et*
580 *al*., 1993; Delvaux *et al*., 1998; Mortimer *et al*., 2007; Macgregor, 2015). Importantly, the
581 range of timings for divergence of the common ancestors of both *F. livingstoni* and *F.*
582 *hanangensis* (4.89-2.63 and 3.25-1.68 Mya respectively; Figure 3) thus may precede the
583 commencement of increased tectonic activity from 2.5 Mya to the present at the MJT. It
584 therefore seems highly likely that this increased faulting and uplift contributed to the

separation of the south central populations of *Fukomys* and East African *F. hanangensis* and *F. livingstoni*, and today this mountainous habitat represents a significant physical barrier to dispersal for a subterranean rodent, with several points (e.g. Rungwe mountain) exceeding 2900 metres above sea level. Interestingly, *F. whytei* populations that diverged a little later are focussed mainly around the MTJ, with the exception of the basal (earlier) Kigogo population that is slightly further east in Tanzania, perhaps arriving when dispersal was easier.

The extensive phylogeographic analysis of *F. hanangensis* and newly acquired *F. livingstoni* samples add further strong support for our earlier assertions (Faulkes *et al*., 2010) that tectonic activity, climatic fluctuations and subsequent expansion and contraction of forest during the Pleiocene-Pleistocene may have also played a role in the sub-structuring of populations and cladogenesis in *Fukomys*. The accompanying Pliocene expansion of C4 grasslands and the savannah habitat in this part of Africa, favoured by mole-rats, would likely have further facilitated range expansion of ancestral populations. The apparently localised and limited distribution of *F. hanangensis* and *F. livingstoni* in Tanzania makes assessment of their conservation status and other aspects of their biology a priority.

Acknowledgements

We are most grateful to Louise Tomsett at the Natural History Museum, London, for help with museum curation and sample preparation, to Kwaku Dakwa for providing the sample from Ghana, and to Dr Dave Hone for comments on the first draft of the manuscript. Thanks also to Judith Chupasko at the Harvard Museum of Comparative Zoology (Department of Mammalogy) for providing photographs of the *F. whytei* skulls collected by Allen & Loveridge (1933), and Marietje Oosthuizen for photographing *F. anselli* skulls collected by Alfred Sichilima.

610 **Data Deposition**

611 Sequence data is deposited in GenBank with Accession numbers as listed in Table 1.

612

References

Aguilar GH. 1993. The karyotype and taxonomic status of *Cryptomys hottentotus darlingi* (Rodentia, Bathyergidae). South African Journal of Zoology **28**: 201–204.

Allard MW, Honeycutt RL. 1992. Nucleotide sequence variation in the mitochondrial 12S rRNA gene and the phylogeny of African mole–rats (Rodentia: Bathyergidae). *Molecular Biology and Evolution* **9**: 27–40.

Allen GM, Loveridge A. 1933. Reports on the scientific results of an expedition to the south–western highlands of Tanganyika Territory. II. Mammals. *Bulletin of the Museum of Comparative Zoology at Harvard* College **75**: 47–140.

Bennett NC, Jarvis JUM, Wallace E. 1990. The relative age structure and body masses of complete wild-captured colonies of the social mole- rats, the common mole-rat, *Cryptomys hottentotus hottentotus* and the Damaraland mole–rat, *Cryptomys damarensis*. *Journal of Zoology* (*London*) **220**: 469–485.

Bennett NC, Jarvis JUM, Cotterill FPD. 1994. The colony structure and reproductive biology of the Mashona mole-rat, *Cryptomys darlingi* from Zimbabwe. *Journal of Zoology, London* **234:** 477–487. DOI: 10.1111/j.1469-7998.1994.tb04861.x

Branchu P, Bergonzini L, Delvaux D, De Batist M, Golubev V, Benedetti M, Klerkx J. 2005. Tectonic, climatic and hydrothermal control on sedimentation and water chemistry of northern Lake Malawi (Nyasa), Tanzania. *Journal of African Earth Sciences* **43**: 433–446.

Burda H, Zima J, Scharff A, Macholán M, Kawalika M. 1999. The karyotypes of *Cryptomys anselli* sp nova and *Cryptomys kafuensis* sp nova: New species of the common mole-rat from Zambia (Rodentia, Bathyergidae). *International Journal of Mammal Biology* **64:** 36–50.

Burda H, Sumbera R, Chitaukali WN, Dryden GL. 2005. Taxonomic status and remarks on ecology of the Malawian mole-rat *Cryptomys whytei* (Rodentia, Bathyergidae). *Acta Theriologica* **50:** 529–536.

Cohen AS, Soreghan MJ, Scholz CA. 1993. Estimating the age of formation of lakes-an example from Lake Tanganyika, East-African Rift System. *Geology* **21:** 511–514.

Chorowicz J. 2005. The East African rift system. *Journal of African Earth Sciences* **43:** 379–410.

Cracraft J. 1989. Speciation and its ontology: The empirical consequences of alternative species concepts for understanding patterns and processes of differentiation. In Otte D, Endler JA, eds. *Speciation and its Consequences*. Sunderland: Sinauer Associates, 28–59.

Davies KTJ, Bennett NC, Tsagkogeorga G, Rossiter SJ, Faulkes CG. 2015. Family Wide Molecular Adaptations to Underground Life in African Mole-Rats Revealed by Phylogenomic Analysis. *Molecular Biology and Evolution*, msv175. http://doi.org/10.1093/molbev/msv175

Delvaux D, Kervyn F, Vittori E, Kajara RSA, Kilembe E. 1998. Late Quarternary tectonic activity and lake level change in the Rukwa Rift Basin. *Journal of African Earth Sciences* **26:** 397–421.

Delvaux D. 1995. Age of Lake Malawi (Nyasa) and water level fluctuations. Musée royal de l'Afrique Centrale (Tervuren). *Département de Géologie et Minéralogie rapport annuel*. 1993(1994): 99–108.

Drummond AJ, Suchard MA, Xie D, Rambaut A. 2012. Bayesian phylogenetics with BEAUti and the BEAST 1.7 *Molecular Biology And Evolution* **29**: 1969–1973.

Drummond AJ, Rambaut A. 2007. BEAST: Bayesian evolutionary analysis by sampling trees. *BMC Evolutionary Biology* **7**: 214.

Drummond AJ, Ho SYW, Phillips MJ, Rambaut A. 2006. Relaxed phylogenetics and dating with confidence. *PLoS Biology* 4, e88

Ebinger CJ, Deino AL, Tesha AL, Becker T, Ring U. 1993. Tectonic Controls on Rift Basin Morphology: Evolution of the Northern Malawi (Nyasa) Rift. *Journal of Geophysical Research* **17**: 821–836.

Faulkes CG, Bennett NC, Bruford MW, O'Brien HP, Aguilar GH, Jarvis JUM. 1997. Ecological constraints drive social evolution in the African mole–rats. *Proceedings of the Royal Society of London Series B, Biological Sciences* **264**: 1619–1627.

Faulkes CG, Verheyen E, Verheyen W, Jarvis JUM, Bennett NC. 2004. Phylogeographical patterns of genetic divergence and speciation in African mole-rats (Family: Bathyergidae). *Molecular Ecology* **13**: 613–629 DOI 10.1046/j.1365-294X.2004.02099.x.

Faulkes C, Mgode GF, Le Comber SC, Bennett NC. 2010. Cladogenesis and endemism in Tanzanian mole-rats, genus *Fukomys*: (Rodentia Bathyergidae): a role for tectonics? *Biological Journal of the Linnean Society* **100**: 337–352 (doi:10.1111/j.1095-8312.2010.01418.x)

Faulkes CG, Bennett NC, Cotterill FPD, Stanley W, Mgode GF, Verheyen E. 2011. Phylogeography and cryptic diversity of the solitary-dwelling silvery mole-rat, genus

Heliophobius (family: Bathyergidae). *Journal of Zoology* **285**:324–338 DOI 10.1111/j.1469-7998.2011.00863.x.

Faulkes CG, Bennett NC. 2013. Plasticity and constraints on social evolution in African mole-rats: ultimate and proximate factors. *Philosophical Transactions of the Royal Society B* **368**:20120347 DOI 10.1098/rstb.2012.0347.

Huchon D, Douzery EJP. 2001. From the Old World to the New World: a molecular chronicle of the phylogeny and biogeography of Hystricognath rodents. *Molecular Phylogenetics and Evolution* **20**:238–251 DOI 10.1006/mpev.2001.0961.

Ingram CM, Burda H, Honeycutt RL. 2004. Molecular phylogenetics and taxonomy of the African mole-rats, genus *Cryptomys* and the new genus *Coetomys* Gray, 1864. *Molecular Phylogenetics and Evolution* **31**:997–1014 DOI 10.1016/j.ympev.2003.11.004.

Kawalika M, Burda H, Bruggert D. 2001. Was Zambia a cradle of the genus *Cryptomys* (Bathyergidae, Rodentia)? In: Denys C, Granjon L, Poulet A, eds. *African small mammals*. Paris: IRD Editions, Collection Colloques et Seminaires, 253–261.

Kock D, Ingram CM, Frabotta LJ, Honeycutt RL, Burda H. 2006. On the Nomenclature of Bathyergidae and *Fukomys* N. Gen. (Mammalia: Rodentia). *Zootaxa* **1142**: 51–55.

Kingdon J, Butynski TM, Happold DCD, Happold M, Hoffmann M. 2013. Mammals of Africa Volume 3: Rodents, hares and rabbits. London: Bloomsbury Publishing.

Lavocat R. 1973. Les rongeurs du Miocene d'Afrique Orientale. I. Miocene Inferieur. *Memoires et Travaux de L'ephe, Institut de Montpellier*, **1**: 1–284.

Macgregor D. 2015. History of the development of the East African Rift System: A series of interpreted maps through time. *Journal of African Earth Sciences* **101:** 232–252 doi.org/10.1016/j.jafrearsci.2014.09.016

Maddison WP, Maddison DR. 2014. Mesquite: a modular system for evolutionary analysis. Version 3.01 http://mesquiteproject.org

Macholan M, Burda H, Zima J, Misek I, Kawalika M. 1993. Karyotype of the giant mole rat, *Cryptomys mechowi* (Bathyergidae, Rodentia). *Cytogenetics* and *Cell Genet*ics **64**: 261–263.

Macholan M, Scharff A, Burda H, Zima J, Grutjen O. 1998. A new karyotype of a common mole-rat and taxonomical status of *Cryptomys amatus* from Zambia. *Zeitschrift Fur Saugetierkunde* **63**: 186–190.

Mortimer E, Paton D, Scholz C, Strecker MR, Blisniuk P. 2007. Orthogonal to oblique rifting: effect of rift basin orientation in the evolution of the North basin, Malawi Rift, East Africa. *Basin Research* **19:** 393–407.

Nevo E, Capanna E, Corti M, Jarvis JUM, Hickman GC. 1986. Karyotype differentiation in the endemic subterranean mole-rats of South Africa (Rodentia: Bathyergidae). *Zeitschrift fur Saugetierkunde* **51:** 6–49.

Rohlf FJ. 2003. *tpsRelw, relative warps analysis version 1.36*. Department of Ecology and Evolution, State University of New York at Stony Brook.

Rohlf FJ. 2004. *tpsUtil, file utility program version 1.26*. Department of Ecology and Evolution, State University of New York at Stony Brook.

Stanley HM. 1872. How I Found Livingstone. Travels, adventures, and discoveries in Central Africa; including four months' residence with Dr. Livingstone. London: Sampson Low.

Swynnerton GH, Hayman RW. 1951. A checklist of the land mammals of the Tanganyika Territory and the Zanzibar Protectorate. *Journal of the East African Natural History Society and National Museum* **20**: 274–392.

Tamura K, Nei M. 1993. Estimation of the number of nucleotide substitutions in the control region of mitochondrial DNA in humans and chimpanzees. *Molecular Biology and Evolution* **10**: 512–526.

Tamura K, Stecher G, Peterson D, Filipski A, Kumar S. 2013. MEGA6: Molecular Evolutionary Genetics Analysis version 6.0. *Molecular Biology and Evolution* **30**: 2725–2729.

Trauth MH, **Maslin MA**, **Deino A**, **Strecker MR. 2005.** Late Cenozoic moisture history of East Africa. *Science* **309:** 2051-2053.

Van Daele PAAG, Blondé P, Stjernstedt R, Adriaens D. 2013. A new species of African Mole-rat (*Fukomys*, Bathyergidae, Rodentia) from the Zaire-Zambezi Watershed. *Zootaxa* **3636:** 171 DOI 10.11646/zootaxa.3636.1.7.

Van Daele PAAG, Verheyen E, Brunain M, Adriaens D. 2007a. Cytochrome *b* sequence analysis reveals differential molecular evolution in African mole–rats of the chromosomally hyperdiverse genus *Fukomys* (Bathyergidae, Rodentia) from the Zambezian region. *Molecular Phylogenetics and Evolution* **45**: 142–157.

782 **Van Daele PAAG, Faulkes CG, Verheyen E, Adriaens D. 2007b.** African mole–rats
783 (Bathyergidae): A complex radiation in Afrotropical soils. In: Begall S, Burda H, Schleich
784 CE, eds. *Subterranean Rodents: News from Underground*. Heidelberg: Springer–Verlag,
785 357–373.
786

787 **Van Daele PAAG, Dammann P, Meier JL, Kawalika M, Van De Woestijne C, Burda H.**
788 **2004.** Chromosomal diversity in mole–rats of the genus *Cryptomys* (Rodentia: Bathyergidae)
789 from the Zambezian region: with descriptions of new karyotypes. *Journal of Zoology* **264**:
790 317–326.
791

792 **Verheyen WN, Colyn M, Hulselmans J. 1996.** Re-evaluation of the *Lophuromys*
793 *nudicaudus* HELLER, 1911 species-complex with a description of a new species from Zaire
794 (Muridae - Rodentia). *Bulletin de l'Institut Royal des Sciences Naturelles de Belgique*
795 *Biologie* **66**: 241–273.
796

797 **Voje KL, Hemp C, Flagstad O, Sætre G-P, Stenseth NC. 2009.** Climatic change as an
798 engine for speciation in flightless Orthoptera species inhabiting African mountains.
799 *Molecular Ecology* **18:** 93–108.
800

801 **Walton AH, Nedbal MA, Honeycutt RL. 2000.** Evidence from Intron 1 of the nuclear
802 transthyretin (prealbumin) gene for the phylogeny of African mole–rats (Bathyergidae).
803 *Molecular Phylogenetics and Evolution* **16**: 467–474.
804

805 **Waterhouse CO. 1841.** Bathyergidae. *The Annals and Magazine of Natural History* **8:** p81.
806

807 **Weiss JD, Cotterill FPD, Schliewen UK. 2015.** Lake Tanganyika—A 'Melting Pot' of
808 Ancient and Young Cichlid Lineages (Teleostei: Cichlidae)? *PLoS ONE* **10:** e0125043 DOI
809 10.1371/journal.pone.0125043.
810

811

Figure 1: (a) Map showing the relative locations of the main *Fukomys* clades considered in this study as defined by Van Daele *et al*. (2007a) and Faulkes *et al*. (2004, 2010, 2011), with letters in circles corresponding as follows (see Figure Y): u: Ujiji; h: Hanang; L: Lufubu clade; W: West Bangweulu clade; E: East Bangweulu clade; v: *F. vandewoestijineae*; m: *F. mechowii*; a: *F. amatus*; mi: *F. micklemi*; an: *F. anselli*; d: *F. damarensis*; k: *F. kafuensis*; dr: *F. darling*i. *F. bocagei* populations are located further west beyond the coverage of this map as indicated. Red circles correspond to the *F. whytei* clade (*F. whytei* and *F. whytei occlusus*), the geographically closest known populations of *Fukomys* to Hanang and Ujiji (Faulkes *et al*., 2010). Red circles with a white dot denote the origin of *F. whytei* samples included in the skull shape analysis. The area encircled by the broken line corresponds to the Mbeya triple junction fault and the Rungwe volcanic province, linking the Rukwa and Malawi rifts. Lower panels show detailed sampling maps for (b) Ujiji and (c) Hanang, indicating the individual catching sites and relative distribution of *cyt b* haplotypes. Map data: (b) Google, DigitalGlobe, (c) Landsat.

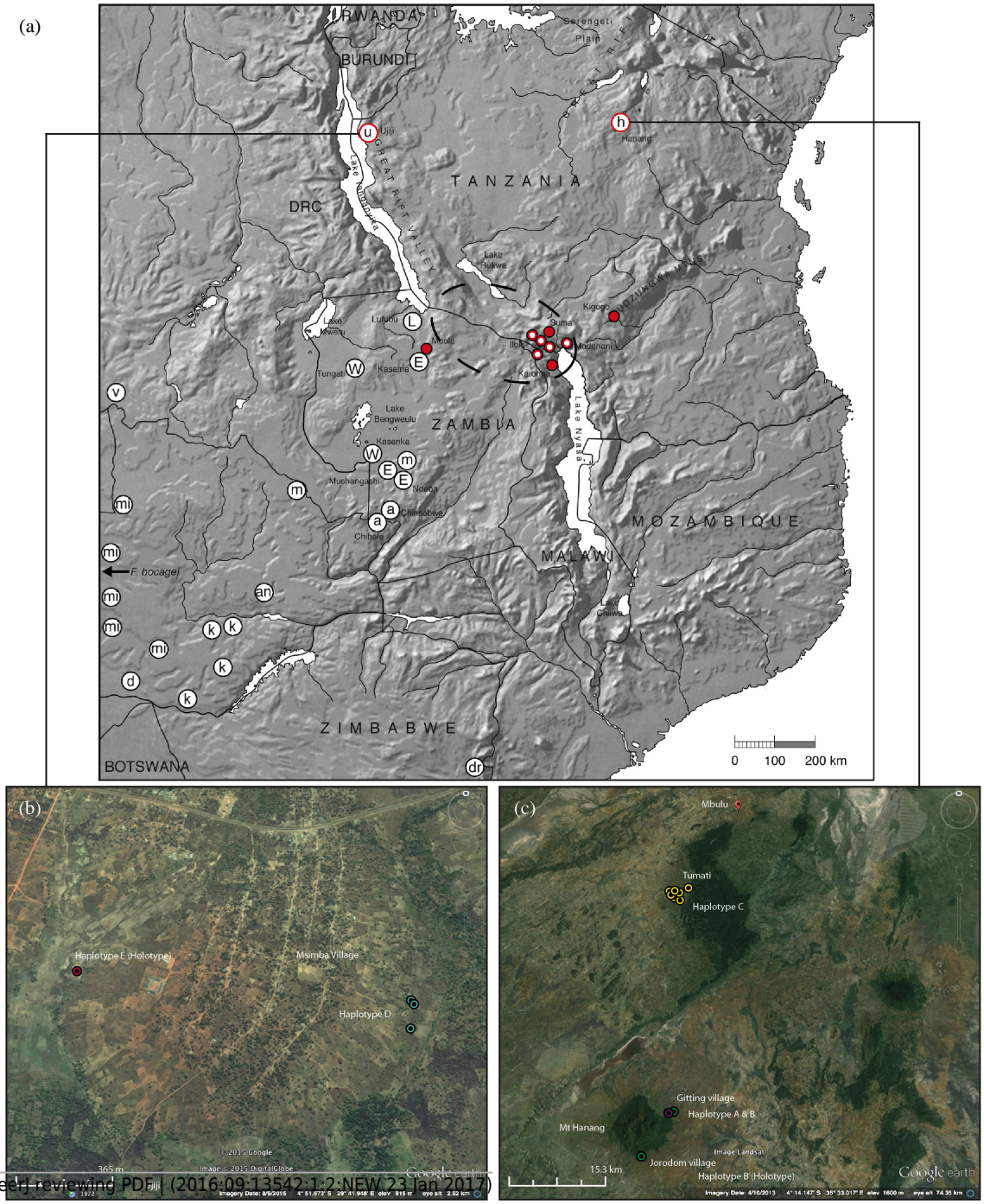

Figure 2 (a) Phylogenetic relationships based on maximum likelihood analysis of 25 cytochrome *b* (*cyt b*) mitochondrial DNA ingroup haplotypes and two outgroups: *Heliophobius* and *Cryptomys hottentotus hottentotus*. Clade descriptors and circular symbols correlate with maps in Figures 1 and 2, while the numbers at each node on the branch refer to the percentage bootstrap values following 100 replications; (b) differences in topology (indicated by red lines) of the four equally parsimonious trees produced from maximum parsimony analysis, for the clade indicated by the symbol • in (a). Haplotypes labeled for *F. livingstoni* and *F. hanangensis sp. nov*. correspond to those cited in the text, Figure 2 and Table 1, other species are designated according to current taxonomic understanding and GenBank Accession Numbers (Van Daele *et al*., 2007a, 2013; Faulkes *et al*., 2010).

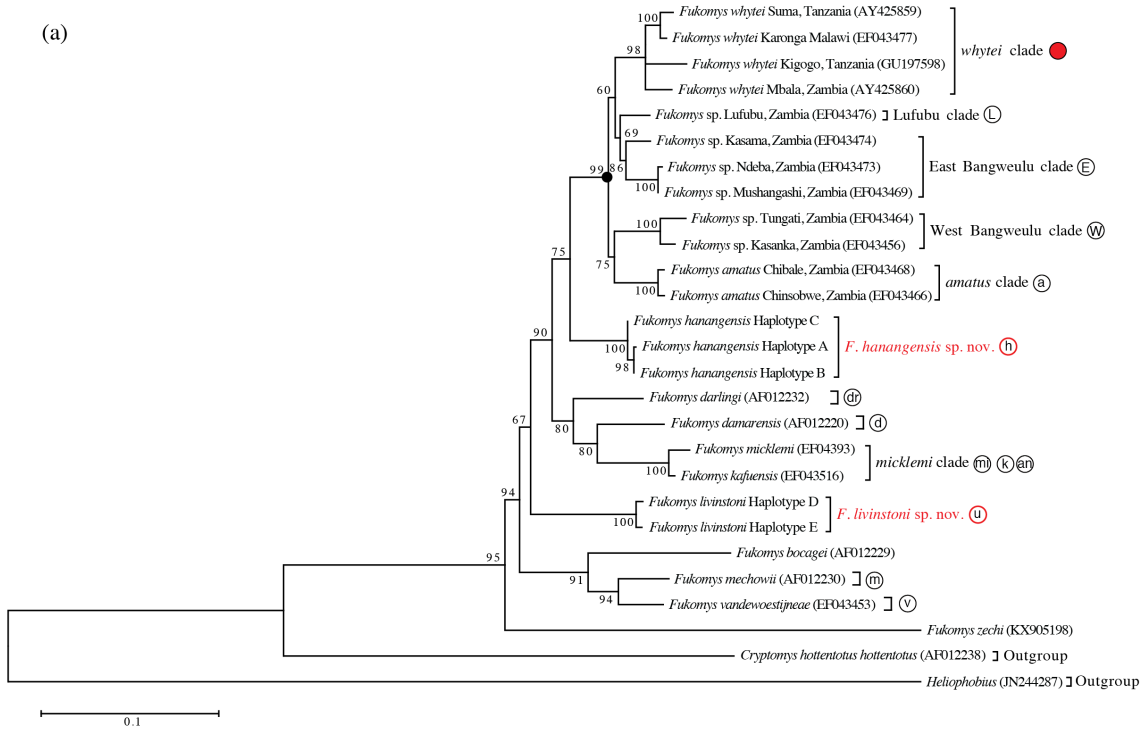
(a)
Fukomys whytei Suma, Tanzania (AY425859)
Fukomys whytei Karonga Malawi (EF043477)
Fukomys whytei Kigogo, Tanzania (GU197598)
Fukomys whytei Mbala, Zambia (AY425860)
whytei clade
Fukomys sp. Lufubu, Zambia (EF043476)
Lufubu clade
Fukomys sp. Kasama, Zambia (EF043474)
Fukomys sp. Ndeba, Zambia (EF043473)
Fukomys sp. Mushangashi, Zambia (EF043469)
East Bangweulu clade
Fukomys sp. Tungati, Zambia (EF043464)
Fukomys sp. Kasanka, Zambia (EF043456)
West Bangweulu clade
Fukomys amatus Chibale, Zambia (EF043468)
Fukomys amatus Chinsobwe, Zambia (EF043466)
amatus clade
Fukomys hanangensis Haplotype C
Fukomys hanangensis Haplotype A
Fukomys hanangensis Haplotype B
F. hanangensis sp. nov.
Fukomys darlingi (AF012232)
Fukomys damarensis (AF012220)
Fukomys micklemi (EF04393)
Fukomys kafuensis (EF043516)
micklemi clade
Fukomys livinstoni Haplotype D
Fukomys livinstoni Haplotype E
F. livinstoni sp. nov.
Fukomys bocagei (AF012229)
Fukomys mechowii (AF012230)
Fukomys vandewoestijneae (EF043453)
Fukomys zechi (KX905198)
Cryptomys hottentotus hottentotus (AF012238)
Outgroup
Heliophobius (JN244287)
Outgroup
0.1

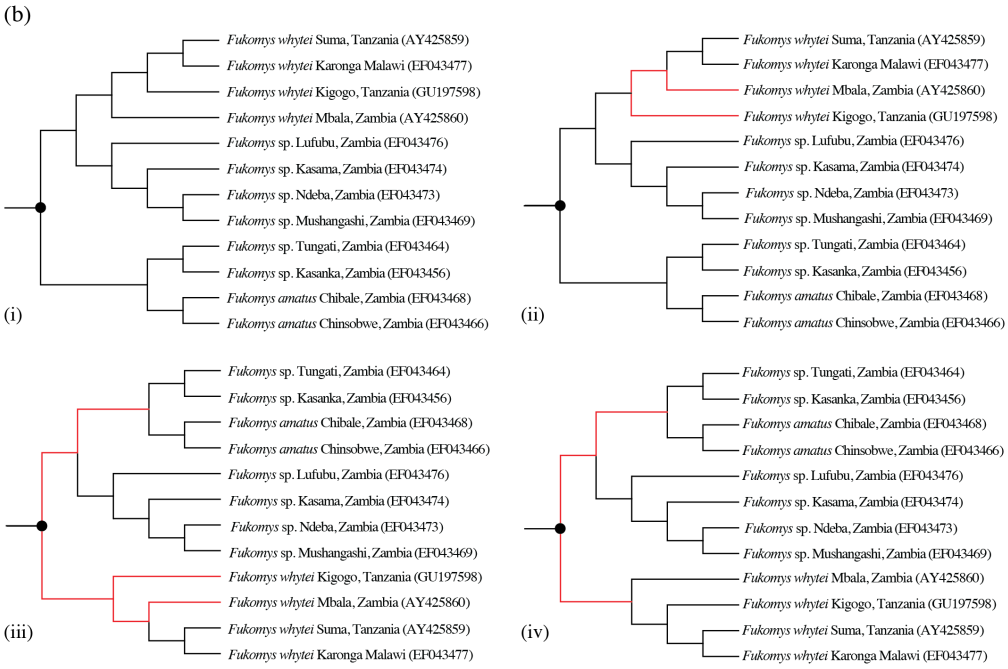
(b)
(i)
Fukomys whytei Suma, Tanzania (AY425859)
Fukomys whytei Karonga Malawi (EF043477)
Fukomys whytei Kigogo, Tanzania (GU197598)
Fukomys whytei Mbala, Zambia (AY425860)
Fukomys sp. Lufubu, Zambia (EF043476)
Fukomys sp. Kasama, Zambia (EF043474)
Fukomys sp. Ndeba, Zambia (EF043473)
Fukomys sp. Mushangashi, Zambia (EF043469)
Fukomys sp. Tungati, Zambia (EF043464)
Fukomys sp. Kasanka, Zambia (EF043456)
Fukomys amatus Chibale, Zambia (EF043468)
Fukomys amatus Chinsobwe, Zambia (EF043466)
(ii)
Fukomys whytei Suma, Tanzania (AY425859)
Fukomys whytei Karonga Malawi (EF043477)
Fukomys whytei Mbala, Zambia (AY425860)
Fukomys whytei Kigogo, Tanzania (GU197598)
Fukomys sp. Lufubu, Zambia (EF043476)
Fukomys sp. Kasama, Zambia (EF043474)
Fukomys sp. Ndeba, Zambia (EF043473)
Fukomys sp. Mushangashi, Zambia (EF043469)
Fukomys sp. Tungati, Zambia (EF043464)
Fukomys sp. Kasanka, Zambia (EF043456)
Fukomys amatus Chibale, Zambia (EF043468)
Fukomys amatus Chinsobwe, Zambia (EF043466)
(iii)
Fukomys sp. Tungati, Zambia (EF043464)
Fukomys sp. Kasanka, Zambia (EF043456)
Fukomys amatus Chibale, Zambia (EF043468)
Fukomys amatus Chinsobwe, Zambia (EF043466)
Fukomys sp. Lufubu, Zambia (EF043476)
Fukomys sp. Kasama, Zambia (EF043474)
Fukomys sp. Ndeba, Zambia (EF043473)
Fukomys sp. Mushangashi, Zambia (EF043469)
Fukomys whytei Kigogo, Tanzania (GU197598)
Fukomys whytei Mbala, Zambia (AY425860)
Fukomys whytei Suma, Tanzania (AY425859)
Fukomys whytei Karonga Malawi (EF043477)
(iv)
Fukomys sp. Tungati, Zambia (EF043464)
Fukomys sp. Kasanka, Zambia (EF043456)
Fukomys amatus Chibale, Zambia (EF043468)
Fukomys amatus Chinsobwe, Zambia (EF043466)
Fukomys sp. Lufubu, Zambia (EF043476)
Fukomys sp. Kasama, Zambia (EF043474)
Fukomys sp. Ndeba, Zambia (EF043473)
Fukomys sp. Mushangashi, Zambia (EF043469)
Fukomys whytei Mbala, Zambia (AY425860)
Fukomys whytei Kigogo, Tanzania (GU197598)
Fukomys whytei Suma, Tanzania (AY425859)
Fukomys whytei Karonga Malawi (EF043477)

Figure 3: Maximum clade credibility tree inferred using BEAST with an uncorrelated relaxed molecular clock model (allowing a variable rate of sequence evolution across the tree). Blue bars spanning nodes correspond to ages for the lower and upper bound of the 95% highest posterior density (HPD) intervals. The clock calibration to convert genetic distance to time is based on calibration 1 (Ingram et al., 2004). Numbers at nodes refer to the posterior probabilities in support of that node (1=100%). A: divergence of *F. livingstoni*, and B: divergence of *F. hanangensis*. Additional palaeoecological, palaeoclimatic and geological annotations are based on Voje et al. (2009), Trauth et al. (2005) and Ebinger et al. (1993), respectively. Circled letters on clade labels correspond to locations on Figure 1, with GenBank accession numbers in parentheses. MJT = corresponds to the period of increased tectonic activity at the Mbeya Triple Junction.

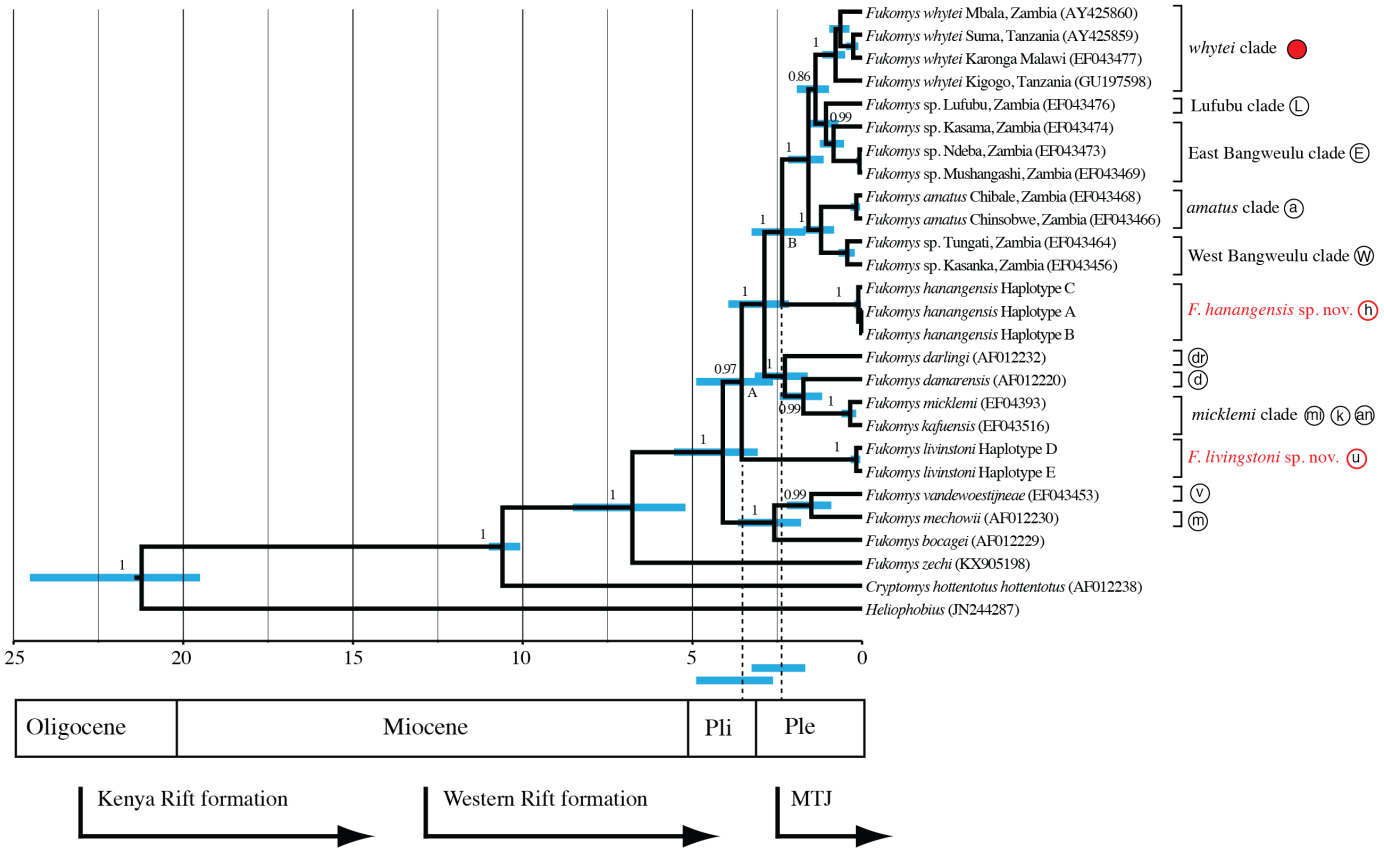

Figure 4: Scatter plot of sample means of relative warp 1 (x-axis) against relative warp 2 (y-axis) from the shape analysis for (a) dorsal, and (b) ventral skull surfaces. Plot symbols squares= males, circles=females, diamonds= sex unknown, *F. hanangensis* animals from Hanang. Colours: orange, *F. livingstoni*; black, *F. hanangensis*; grey, *F. whytei*; dark purple, *F. anselli*. Circled *F. hanangensis* outlier is animal 4332, a very small 35g male (Table S1).

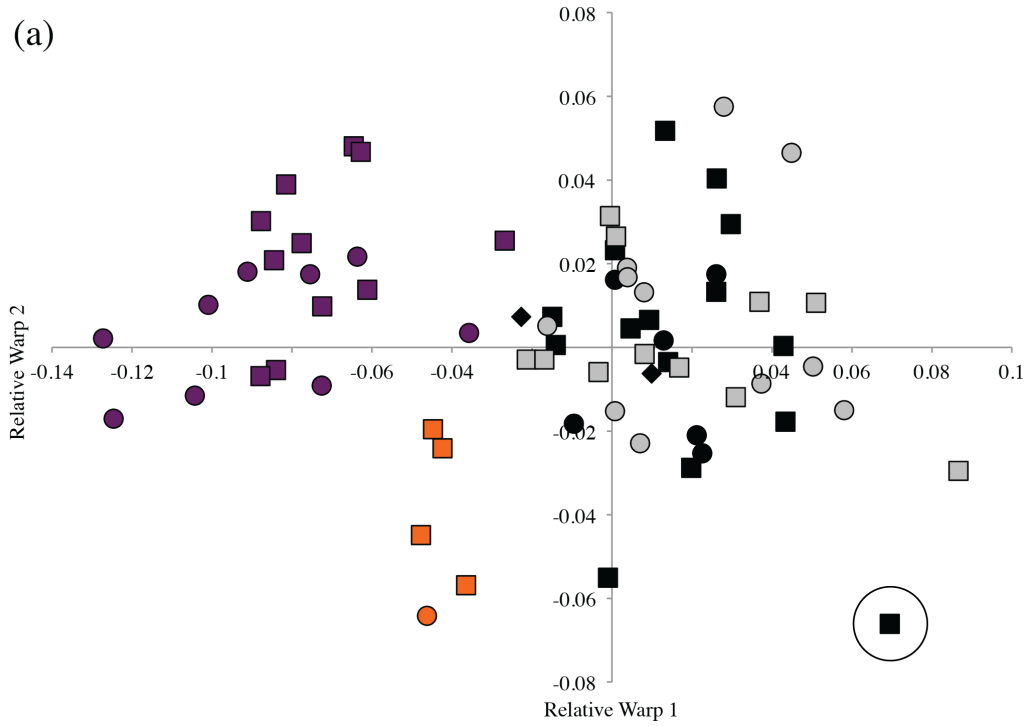

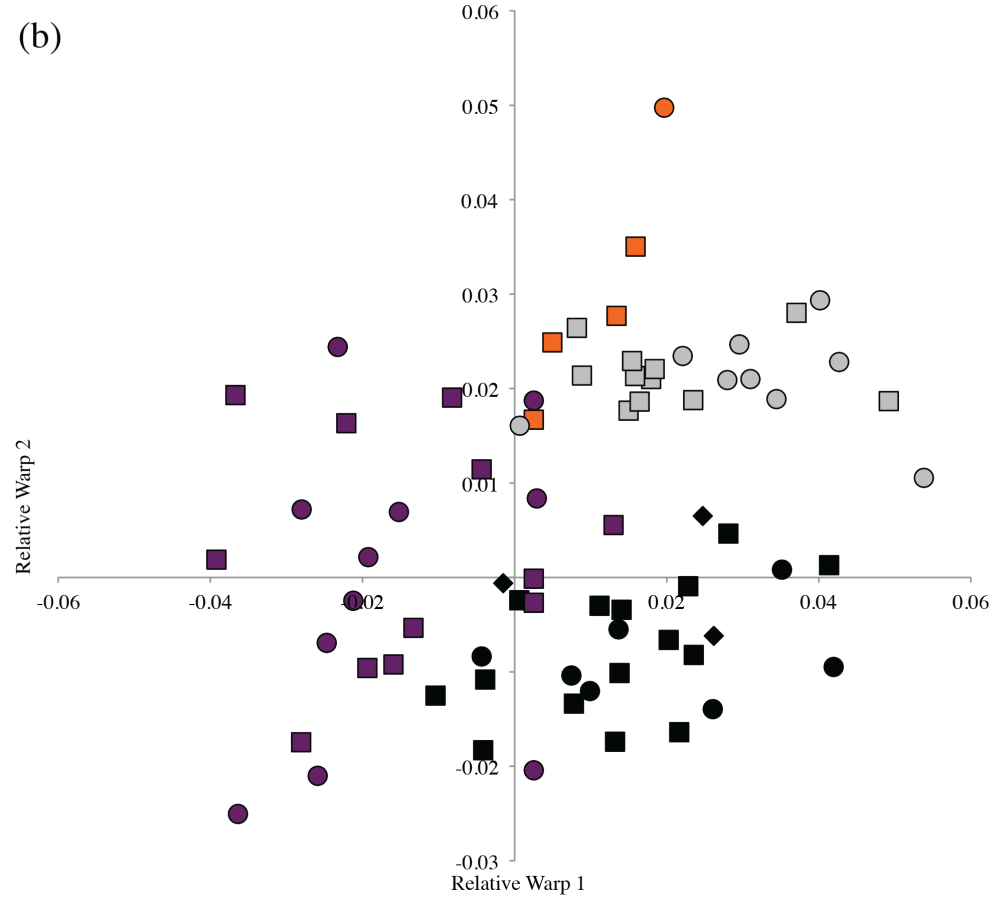

Figure 5: Dorsal (a) and (c) and ventral (b) and (d) views of holotypes: *Fukomys livingstoni* (5208/NHMUK 2015.42) (a) and (b) and *Fukomys hanangensis* (4308/NHMUK 2015.15), (c) and (d). Scale bar = 1cm

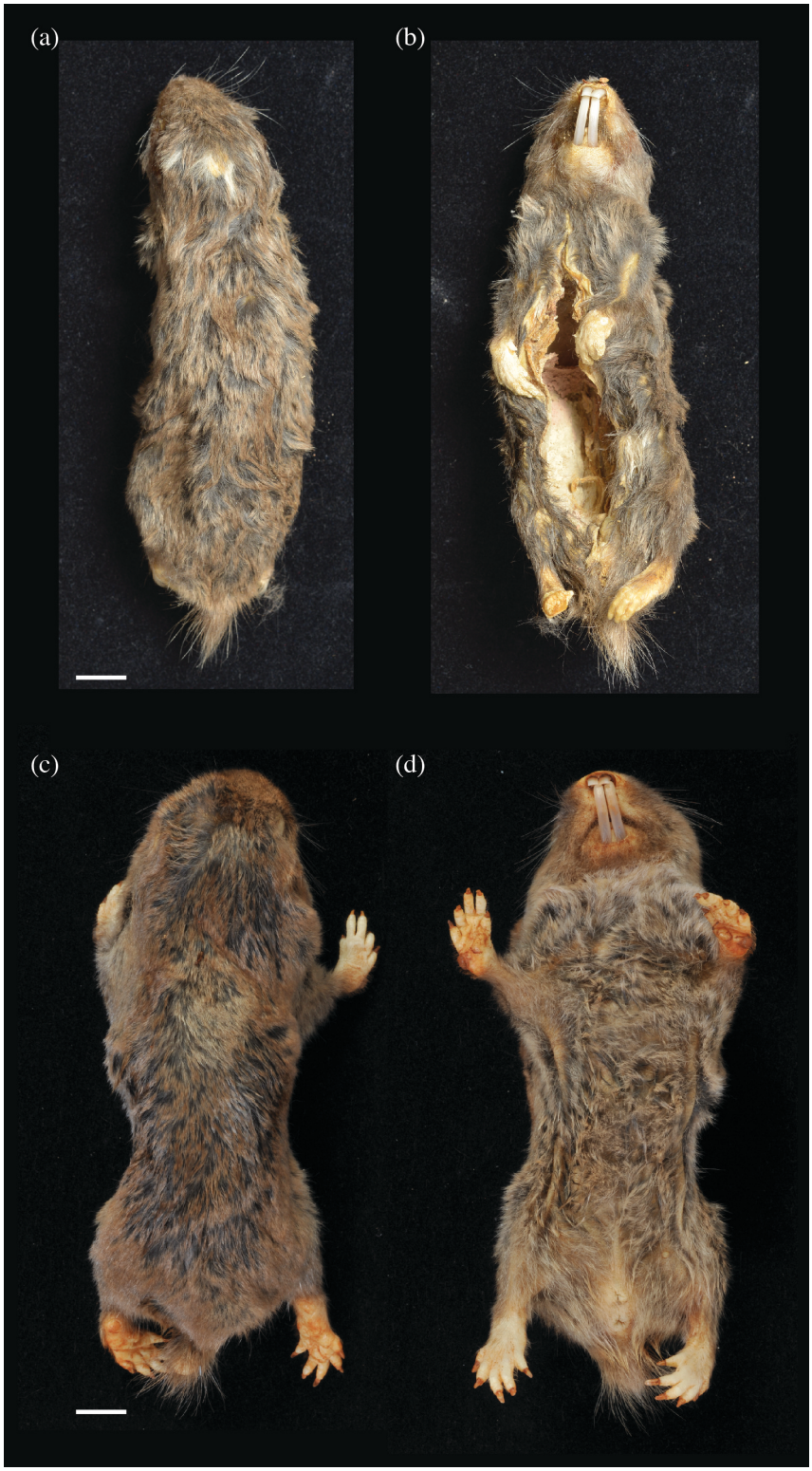

Figure 6. Skulls of (a) *Fukomys livingstoni* sp. nov. (5208/NHMUK 2015.42; holotype), and (b) *Fukomys hanangensis* sp. nov. (4334/NHMUK 2015.41; paratype) in dorsal, ventral and lateral view, and mandible in lateral and dorsal view.

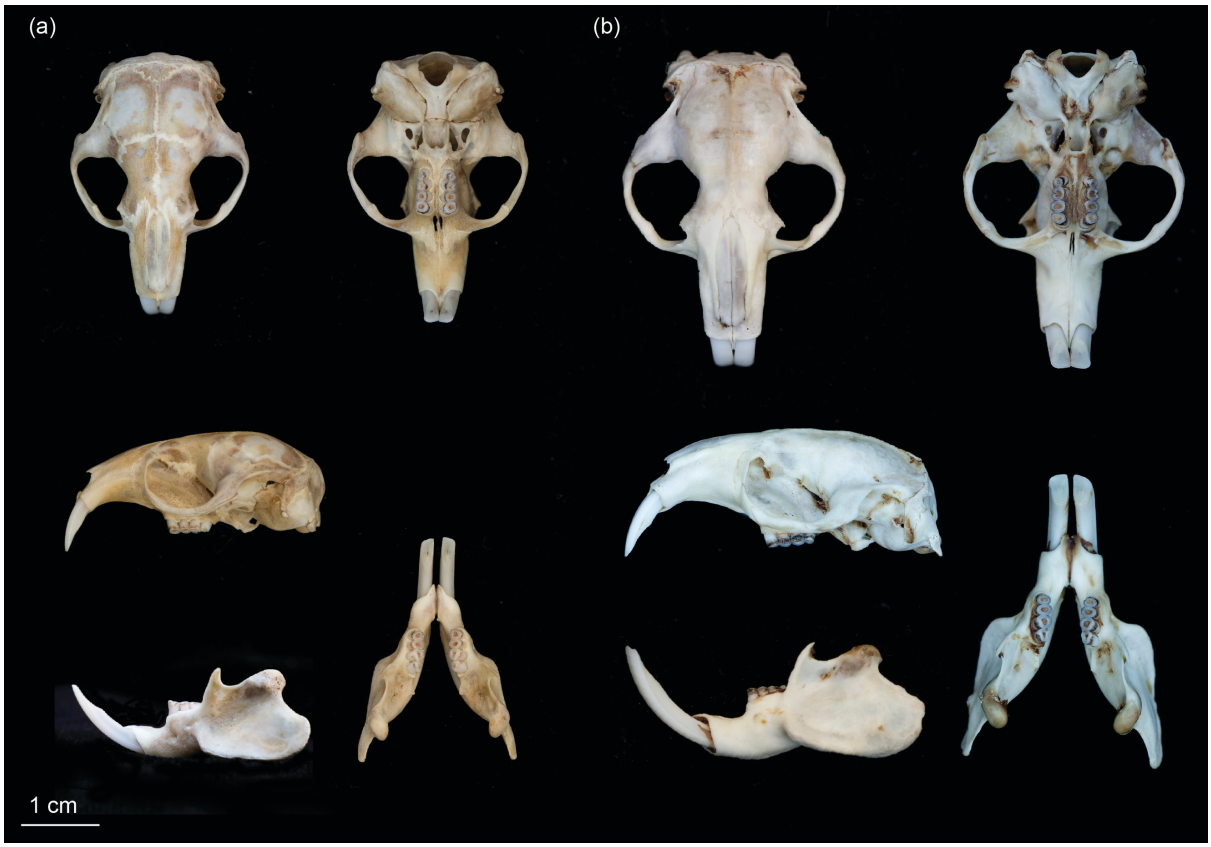

Table 1 - Collection and sample data for *F. hanangensis*, *F. livingstoni* and *F. whytei*, together with Genbank Accession numbers and the respective haplotype (hapl.) for *cyt b* sequences. QMUL: Queen Mary, University of London, refers to institutionally archived samples.

		Sample no	Sample		GPS		Altitude			bw	Age	GenBank	*cyt b*	
Species	**QMUL**	**NHM London**	**type**	**Location**	**Lat**	**Long**	**(m)**	**Colony**	**Sex**	**(g)**	**class**	**Accession no**	**hapl.**	**Specimen**
F. hanangensis	3926	–	QMUL	Hanang	S 04° 24'	E 035° 27'	na	na	na	na	2	GU197596	A	skull & tissue
F. hanangensis	3927	–	QMUL	Hanang	S 04° 24'	E 035° 27'	na	na	na	na		GU197595	B	tissue only
F. hanangensis	3928	–	QMUL	Hanang	S 04° 29'	E 035° 24'	1964	na	na	na	2	–	–	skull & tissue
F. hanangensis	4303	NHMUK 2015.14	Paratype	Hanang	S 04° 25.761'	E 035° 27.158'	1896	1	M	40		KX905166	B	whole animal
F. hanangensis	4304	–	QMUL	Hanang	S 04° 25.761'	E 035° 27.158'	1896	1	F	50		KX905167	B	whole animal
F. hanangensis	4305	–	QMUL	Hanang	S 04° 25.412'	E 035° 27.453'	1856	2	M	120		KX905168	B	tissue only
F. hanangensis	4306	–	QMUL	Hanang	S 04° 25.412'	E 035° 27.453'	1856	2	na	na		KX905169	B	tissue only
F. hanangensis	4307	–	QMUL	Hanang	S 04° 25.412'	E 035° 27.453'	1856	2	na	50		KX905170	B	tissue only
F. hanangensis	4308	NHMUK 2015.15	Holotype	Hanang	S 04° 29.510'	E 035° 24.519'	1957	1	BrF	62		KX905171	B	whole animal
F. hanangensis	4309	NHMUK 2015.16	Paratype	Mbulu	S 04° 3.165'	E 035° 26.430'	2135	2	F	57	2	KX905172	C	skull & tissue
F. hanangensis	4310	NHMUK 2015.17	Paratype	Mbulu	S 04° 2.591'	E 035° 27.511'	2188	2	F?	80	3	KX905173	C	skull & tissue
F. hanangensis	4311	NHMUK 2015.18	Paratype	Mbulu	S 04° 2.591'	E 035° 27.511'	2188	2	M	68	2	KX905174	C	skull & tissue
F. hanangensis	4312	NHMUK 2015.19	Paratype	Mbulu	S 04° 2.591'	E 035° 27.511'	2188	2	M?	55	2	KX905175	C	skull & tissue
F. hanangensis	4313	NHMUK 2015.20	Paratype	Mbulu	S 04° 2.591'	E 035° 27.511'	2188	2	F	47	1	KX905176	C	skull & tissue
F. hanangensis	4314	NHMUK 2015.21	Paratype	Mbulu	S 04° 4.091'	E 035° 26.668'	2180	3	M	140		–	–	whole animal
F. hanangensis	4315	NHMUK 2015.22	Paratype	Mbulu	S 04° 4.091'	E 035° 26.668'	2180	3	M?	85	2	KX905177	C	skull & tissue
F. hanangensis	4316	NHMUK 2015.23	Paratype	Mbulu	S 04° 4.091'	E 035° 26.668'	2180	3	F	54	1	KX905178	C	skull & tissue
F. hanangensis	4317	NHMUK 2015.24	Paratype	Mbulu	S 04° 4.091'	E 035° 26.668'	2180	3	M?	65	3	KX905179	C	skull & tissue
F. hanangensis	4318	NHMUK 2015.25	Paratype	Mbulu	S 04° 3.528'	E 035° 26.189'	2179	4	F	60		–	–	whole animal
F. hanangensis	4319	NHMUK 2015.26	Paratype	Mbulu	S 04° 3.528'	E 035° 26.189'	2179	4	M	100		–	–	whole animal
F. hanangensis	4320	NHMUK 2015.27	Paratype	Mbulu	S 04° 3.528'	E 035° 26.189'	2179	4	M	103	3	KX905180	C	skull & tissue
F. hanangensis	4321	NHMUK 2015.28	Paratype	Mbulu	S 04° 3.528'	E 035° 26.189'	2179	4	M	85		–	–	whole animal
F. hanangensis	4322	NHMUK 2015.29	Paratype	Mbulu	S 04° 3.528'	E 035° 26.189'	2179	4	F	79	3	KX905181	C	skull & tissue
F. hanangensis	4323	NHMUK 2015.30	Paratype	Mbulu	S 04° 3.528'	E 035° 26.189'	2179	4	F	75	3	KX905182	C	skull & tissue
F. hanangensis	4324	NHMUK 2015.31	Paratype	Mbulu	S 04° 3.528'	E 035° 26.189'	2179	4	M	60	2	–	–	skull & tissue
F. hanangensis	4325	NHMUK 2015.32	Paratype	Mbulu	S 04° 3.528'	E 035° 26.189'	2179	4	M	35	1	–	–	skull & tissue
F. hanangensis	4326	NHMUK 2015.33	Paratype	Mbulu	S 04° 2.818'	E 035° 26.029'	2115	5	M	130	3	KX905183	C	skull & tissue
F. hanangensis	4327	NHMUK 2015.34	Paratype	Mbulu	S 04° 2.818'	E 035° 26.029'	2115	5	M	75	1	KX905184	C	skull & tissue
F. hanangensis	4328	NHMUK 2015.35	Paratype	Mbulu	S 04° 2.818'	E 035° 26.029'	2115	5	M	130		–	–	whole animal
F. hanangensis	4329	NHMUK 2015.36	Paratype	Mbulu	S 04° 2.818'	E 035° 26.029'	2115	5	M?	60	2	KX905185	C	skull & tissue

F. hanangensis	4336	–	QMUL	Mbulu	S 04° 3.793'	E 035° 26.294'	2163	7	M	55	1	KX905189	C	skull & tissue
F. hanangensis	4337	–	QMUL	Mbulu	S 04° 3.793'	E 035° 26.294'	2163	7	F	87		–	–	whole animal
F. hanangensis	4338	–	QMUL	Mbulu	S 04° 3.793'	E 035° 26.294'	2163	7	M	130	3	KX905190	C	skull & tissue
F. hanangensis	4339	–	QMUL	Mbulu	S 04° 3.793'	E 035° 26.294'	2163	7	M	115	3	KX905191	C	skull & tissue
F. livinstoni	5208	NHMUK 2015.42	Holotype	Ujiji	S 04° 51.760'	E 028° 42.326'	2601	1	M	50	2	KX905192	D	whole animal
F. livinstoni	5209	NHMUK 2015.43	Paratype	Ujiji	S 04° 51.760'	E 028° 42.326'	2601	1	F	35	1	KX905193	D	skull & tissue
F. livinstoni	5210	NHMUK 2015.44	Paratype	Ujiji	S 04° 51.693'	E 029° 42.335'	2624	2?	F	80	4	KX905194	D	skull & tissue
F. livinstoni	5211	NHMUK 2015.45	Paratype	Ujiji	S 04° 51.701'	E 029° 42.340'	2620	3?	M	42	1	KX905195	D	skull & tissue
F. livinstoni	5212	NHMUK 2015.46	Paratype	Ujiji	S 04° 51.760'	E 028° 42.326'	2601	1	M	38	2	KX905196	D	whole animal
F. livinstoni	5213	NHMUK 2015.47	Paratype	Ujiji	S 04° 51.620'	E 029° 41.542'	2601	4	M	52	2	KX905197	E	whole animal
F. whytei	3913	–	QMUL	Kigogo	S 08° 37.905'	E 035° 12.2754'	1970	1	F	101	1	GU197597	W-A	skull & tissue
F. whytei	3915	–	QMUL	Kigogo	S 08° 38.3442'	E 035° 11.7912'	1946	2	M	134	3	GU197599	W-B	skull & tissue
F. whytei	3916	–	QMUL	Kigogo	S 08° 38.1516'	E 035° 12.5676'	na	3	F	124	3	GU197600	W-A	skull & tissue

Table 2. Mean *cyt b* genetic distances between sequences for each haplotype (%). Below diagonal are uncorrected *p* distances, above diagonal Tamura-Nei + Gamma (1.4964) corrected rates of substitutions.

	1	2	3	4	5	6	7	8	9	10	11	12	13	14	15	16
1. *whytei* clade	–	4.3	4.8	6.3	5.9	7.3	9.5	9.8	10.3	11.6	12.5	12.3	11.8	18.9	25.9	30.4
2. Lufubu_clade	4.0	–	3.4	5.0	5.1	7.0	8.2	9.2	10.2	10.0	12.7	10.9	11.0	19.6	23.8	29.4
3. East Bangweulu clade	4.5	3.3	–	5.7	5.4	7.2	9.0	9.8	9.9	10.7	12.8	11.2	11.0	20.3	23.8	30.5
4. West Bangweulu clade	5.7	4.6	5.2	–	5.7	8.4	9.3	11.3	10.7	11.1	13.7	11.3	11.4	19.7	25.7	31.0
5. *F. amatus* clade	5.4	4.7	4.9	5.2	–	7.9	9.7	10.2	11.2	9.8	12.6	11.2	11.7	20.0	24.9	29.9
6. *F. hanangensis*	6.5	6.3	6.4	7.4	7.0	–	8.2	8.5	9.1	9.9	13.7	12.1	11.9	18.5	24.3	31.6
7. *F. darlingi*	8.2	7.3	7.9	8.0	8.3	7.3	–	7.6	8.0	10.3	14.2	11.7	10.7	18.5	27.4	31.3
8. *F. damarensis*	8.5	8.0	8.5	9.6	8.8	7.5	6.8	–	7.1	11.1	12.9	12.8	13.2	19.5	25.1	28.6
9. *F. micklemi* clade	8.8	8.8	8.5	9.1	9.5	8.0	7.1	6.4	–	10.5	14.1	13.4	12.9	19.7	27.1	29.7
10. *F. livingstoni*	9.7	8.6	9.1	9.4	8.5	8.5	8.8	9.5	8.9	–	13.3	11.4	11.3	18.8	24.8	28.5
11. *F. bocagei*	10.5	10.7	10.7	11.3	10.5	11.3	11.6	10.7	11.5	11.0	–	9.3	10.2	22.5	22.4	30.1
12. *F. mechowii*	10.3	9.3	9.6	9.6	9.6	10.1	9.9	10.7	11.0	9.7	8.1	–	4.8	21.2	29.5	32.2
13. *F. vandewoestijneae*	9.9	9.3	9.3	9.6	9.8	9.9	9.1	10.9	10.5	9.5	8.8	4.5	–	21.1	26.9	31.7
14. *F. zechi*	14.6	15.1	15.5	15.1	15.3	14.5	14.5	15.1	15.1	14.5	16.6	16.0	15.8	–	28.3	31.8
15. Outgroup 1	18.2	17.3	17.3	18.1	17.8	17.7	19.0	18.0	18.8	17.8	16.8	20.0	18.7	19.7	–	30.7
16. Outgroup 2	21.5	21.1	21.6	21.8	21.4	22.2	22.0	20.8	21.3	20.5	21.5	22.4	22.1	22.3	21.6	–